Supplementary Video 1 l A tendon fascicle at baseline (unstretched condition), showing sparse spontaneous Ca^{2+} signals in tenocytes. See also corresponding Fig. 1b,c.

Supplementary Video 2 l A tendon fascicle during tissue stretching from 0–10% strain, showing a tissue-wide Ca^{2+} response in tenocytes. See also corresponding Fig. 1b,c.

Supplementary Video 3 l Propagation of Ca^{2+} signals to neighbouring cells, potentially through cell–cell communication.

Supplementary Video 4 l Isolated human tenocytes showing Ca^{2+} signals on stimulation with 5-Pa shear stress. See also corresponding Fig. 2d.

Supplementary Video 5 l A tendon fascicle stimulated with the PIEZO1-agonist Yoda1, showing a prompt Ca^{2+} response in tenocytes. See also corresponding Supplementary Fig. 6g.

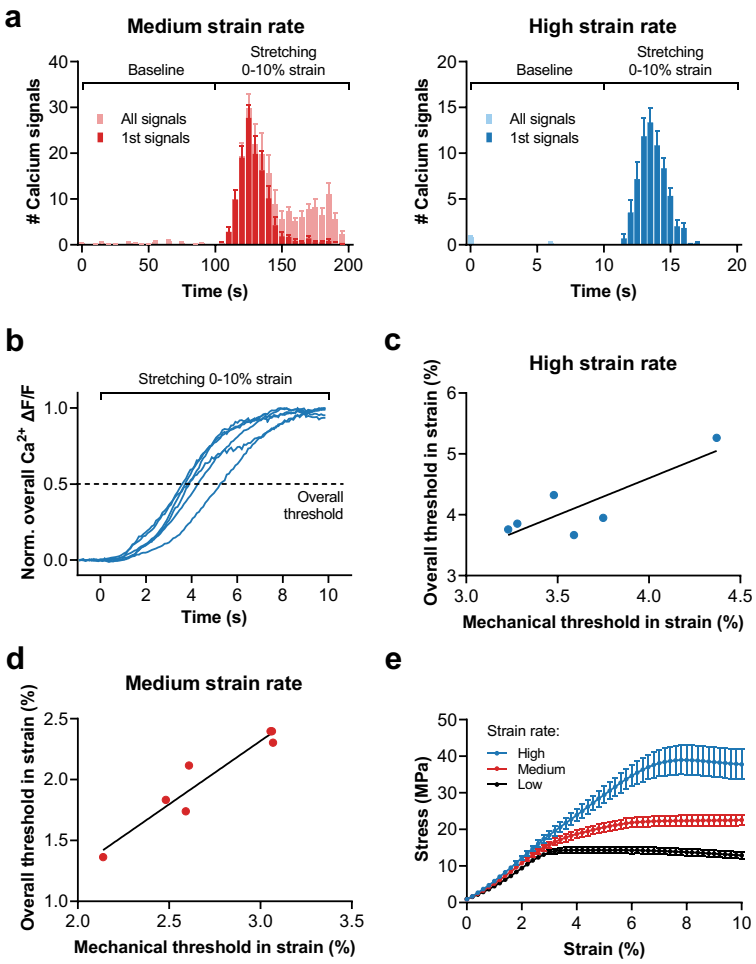

Supplementary Fig. 1 | The mechanosensitive Ca^{2+} response in tendon explants and the normalized overall change in fluorescence intensity as an estimate of the mechanical threshold. a, Quantification of intracellular Ca^{2+} elevations during stretching protocols from 0-10% strain at medium strain rate (0.1% strain/s, n=7 fascicles) and high strain rate (1.0% strain/s, n=6 fascicles). **b**, The overall change in Ca^{2+} fluorescence intensity (normalized to the maximum intensity) of tendon fascicles stretched at high strain rate. **c**, Significant correlation between the overall threshold and the mechanical threshold for the high strain rate data ($y = 1.212\ x - 0.249$; $R^2 = 0.715$; $p = 0.034$) and (**d**) the medium strain rate data ($y = 1.041\ x - 0.805$; $R^2 = 0.913$; $p<0.001$). Hence, mechanical thresholds can be estimated with the overall threshold, which represents a straightforward approach. **e**, The mechanical data corresponding to the Ca^{2+} imaging experiments (see Fig. 1c and d) with tendon fascicles stretched at low, medium and high strain rate. Replicates are biological. Data are means±SEM.

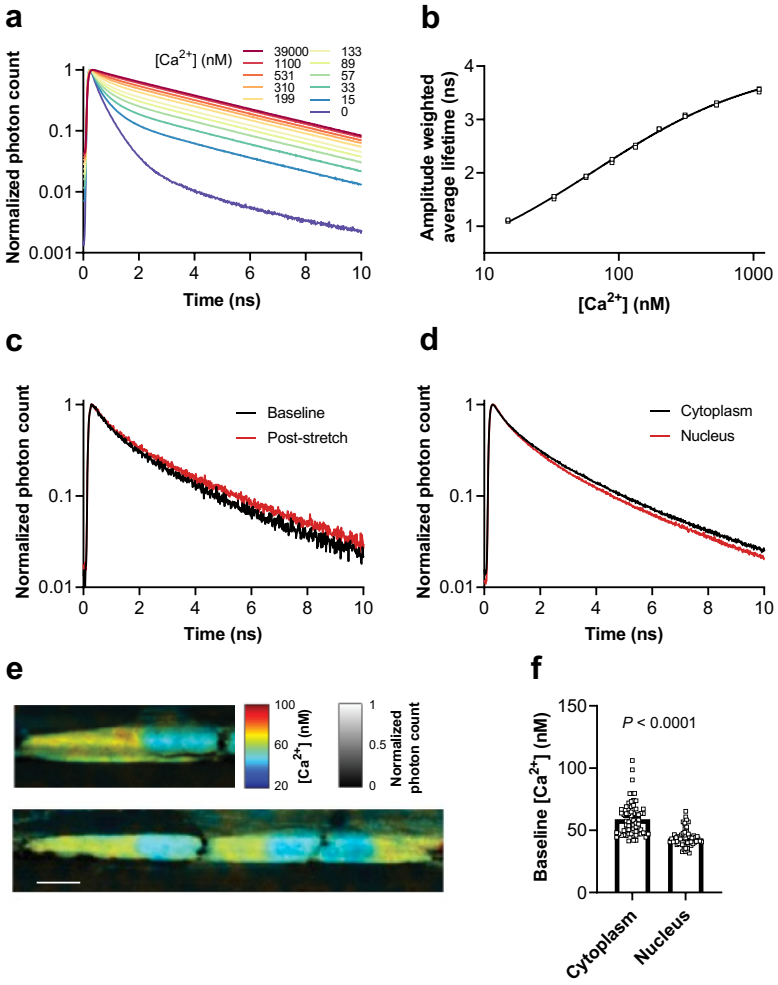

Supplementary Fig. 2 | The OGB-1 FLIM calibration and the characterization of baseline [Ca²⁺] in tenocytes. a, Normalized fluorescent lifetime decays of OGB-1 in calibration solutions at different [Ca²⁺]. **b**, The OGB-1 FLIM readout, obtained from a double-exponential tailfit of the lifetime decays and a subsequent nonlinear fitting with Hill slope of the amplitude weighted average lifetime ($y = \frac{4.074\,x^h}{65.87^h + x^h}$; h = 0.6935 ; R^2 = 0.998). **c**, Representative example of the normalized fluorescent lifetime decay measured in a tenocyte at baseline and post-stretch. Corresponding quantification is shown in Figure 1g. **d**, Subcellularly measured normalized fluorescent lifetime decays of a representative quiescent tenocyte. Corresponding quantification is shown in panel f. **e**, Heterogenous landscape of resting [Ca²⁺] in tenocytes (scale bar, 10 µm). **f**, Subcellular quantification of [Ca²⁺] in quiescent tenocytes (n=66 cells from 8 fascicles), paired Student's t-test. Replicates are biological. Data are means±SEM.

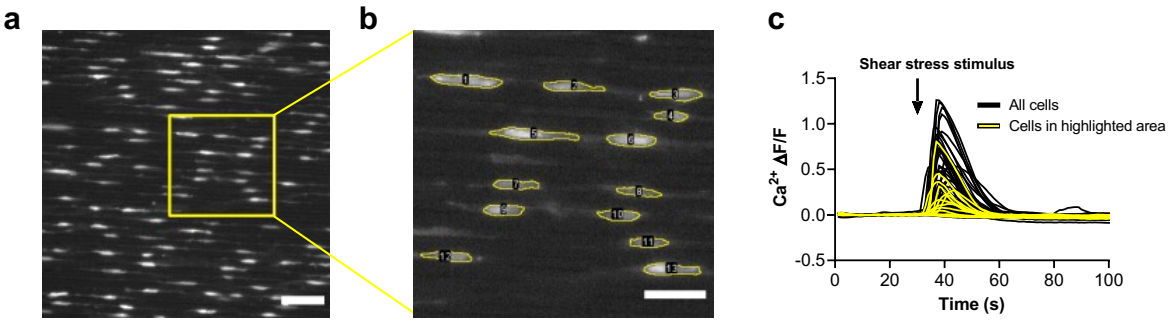

Supplementary Fig. 3 | Analysis of Ca^{2+} images from shear stress experiments. a, Entire field of view showing tenocytes seeded in the flow chamber and stained with Fluo-4 (scale bar, 100 µm). **b**, Segmentation of single cells (scale bar, 50 µm). **c**, Corresponding time traces of the fluorescence signals measured in the single segmented cells.

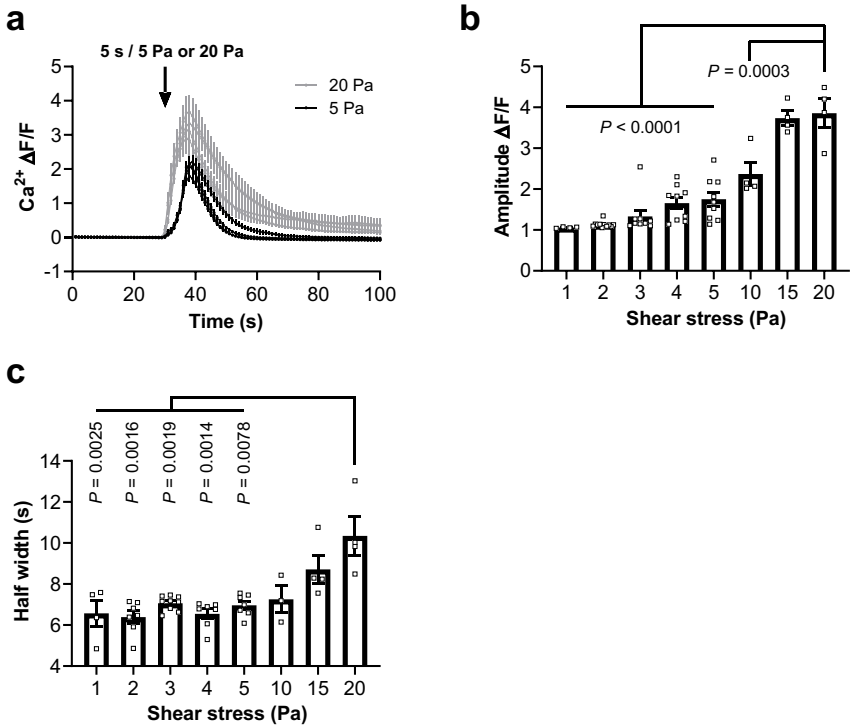

Supplementary Fig. 4 | Magnitude dependency of the shear stress response in human tenocytes. a, Time traces of Ca^{2+} signals induced by 5 Pa or 20 Pa shear stress. **b**, Median amplitude and (**c**) duration of the Ca^{2+} signals depend on the magnitude of shear stress stimulus (for each condition n≥4 chambers, cells from human flexor digitorum tendons), one-way ANOVA with multiple comparisons (Tukey's test). Replicates are biological. Data are means±SEM.

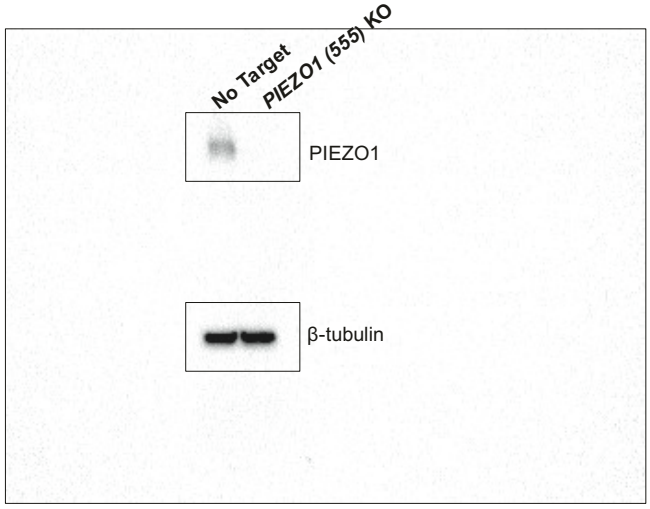

Supplementary Fig. 5 l Full scan of the Western blot shown in Fig. 3d.

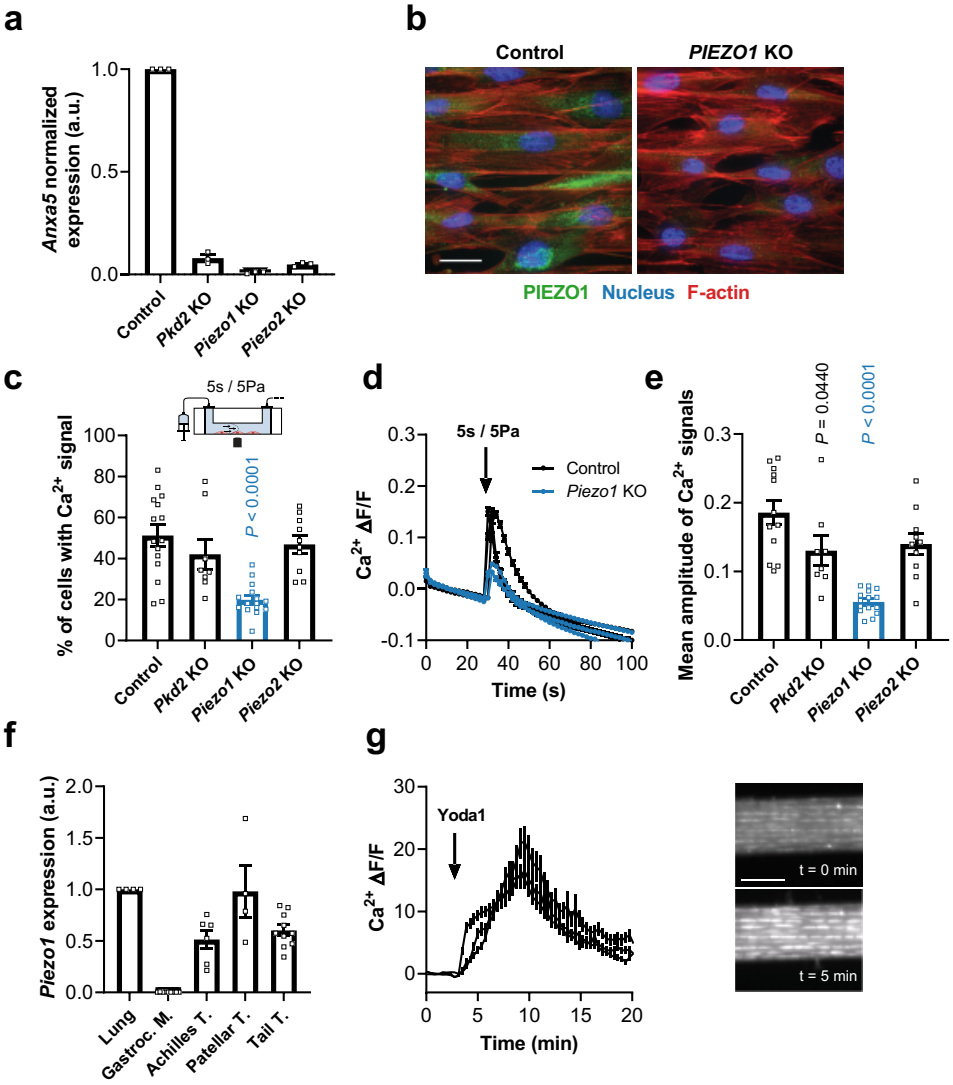

Supplementary Fig. 6 | PIEZO1-mediated shear stress response of rat tenocytes. a, Efficient CRISPR/Cas9-induced knockouts of the candidate genes. Quantitative PCR with a normalization to the expression of the corresponding gene in the control cells using the 2^{-ddCT} method (data from n=3 separate trials, cells from 3 rats) shows a significant reduction ($P < 0.0001$) for all candidates, one-way ANOVA with multiple comparisons (Dunnett's test). **b**, Immunofluorescence images of control and *Piezo1* knockout tenocytes (scale bar, 20 µm). **c-e**, *Piezo1* knockout tenocytes show a reduced % of cells responding to shear stress (5 Pa for 5 s) and a diminished intracellular Ca^{2+} response (averaged over all single segmented cells). For each condition n≥8 chambers were tested with cells from 3 rats, one-way ANOVA with multiple comparisons, (Dunnett's test). **f**, mRNA expression profile of *Piezo1* examined with quantitative PCR in various rat tissues including lung, muscle and tendons. Normalization to the lung, which was reported as one of the body organs with highest *Piezo1* expression[16], using the 2^{-ddCT} method. *Gapdh* was the reference gene (data from n=3 separate trials, 3 rats). **g**, Intracellular Ca^{2+} time traces (averaged over all detected Ca^{2+} signals) in tendon fascicles stimulated with 50 µM PIEZO1-agonist-Yoda1 (n=3 fascicles). Onset of the Yoda1-stimulus is indicated by the arrow. Scale bar, 100 µm. Replicates are biological. Data are means±SEM.

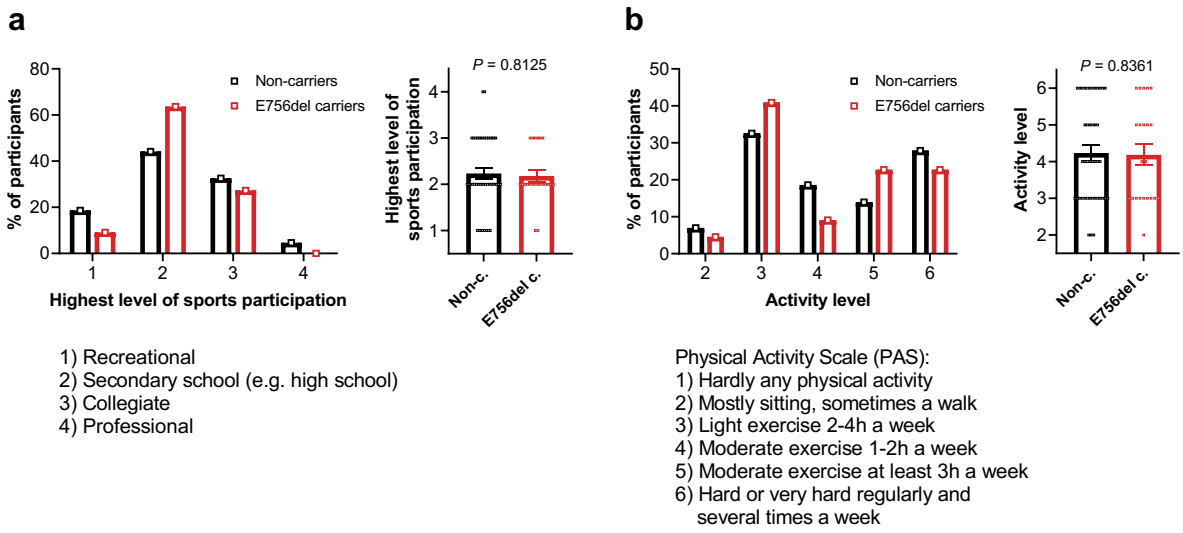

Supplementary Fig. 7 | Similar levels of sports participation and physical activity between E756del carriers and non-carriers. a, No difference in highest level of sports participation between the two groups. **b**, No difference in current activity level assessed with the Physical Activity Scale (PAS). Mann-Whitney test, n=22 E756del carriers and n=43 non-carriers. Replicates are biological. Data are means±SEM.

Supplementary Table 1 | sgRNAs used for human and rat CRISPR/Cas9-mediated knockouts.

Target	sgRNA Target Sequence
PIEZO1 (hu) 395 - 417	CCTTGGAGGCCGCATCGGGT
PIEZO1 (hu) 555-577	GACCCCTATGTGTCGCGAGA
PIEZO1 (hu) 786 - 808	CAGCCGTGACCTCCGTGTAG
PIEZO2 (hu) 1335-1357	GGTAATGGGTTGCGTACCAC
PKD2 (hu) 245-267	AGATCGAGATGCAGCGCATC
TMEM63A (hu) 701-723	TTGTAGCAATAGGAGTCGTT
TMEM63B (hu) 495-517	CAGAGGTGAGACGCTCATAC
TRPC1 (hu) 997-1019	GAGGCTCGTCACTAGACGTA
TRPM7 (hu) 1686-1708	CTTCCAGTCTCGGAATGGTA
TRPV4 (hu) 739-761	CGGAGCGCACCGGCAACATG
Hu Non-Targeting 40	GACTTATAAACTCGCGCGGA
Piezo1 (rat) 840-862	TGCGCCGTGATCCGGAAGCG
Piezo2 (rat) 479-501	CGTGTCTGGGCGGCGTAGTC
Pkd2 (rat) 243-265	GGCATGGAGCCGCGACAACC

Supplementary Table 2 | Forward and reverse primer sequences used for real-time PCR.

Forward Primer	Forward Primer Sequence	Reverse Primer	Reverse Primer Sequence
hu PIEZO1-269-F	GTGCTCGGCGCGGTC	hu PIEZO1-412-R	GAGGCCGCATCGGGTG
hu PIEZO1-490-F	GATCTGCCTGCATATTGTGCC	hu PIEZO1-573-R	CCTATGTGTCGCGAGAGGG
hu PIEZO1-708-F	ATCCACGGGAGCTGGATGAT	hu PIEZO1-807-R	AGCCGTGACCTCCGTGTAG
hu PIEZO2-1256-F	TGCAGGATGAGGGGACCAAA	hu PIEZO2-1356-R	GTAATGGGTTGCGTACCACAG
hu PKD2-960-F	GTACTGGAAGATGCAGCCCA	hu PKD2-1063-R	CTCGGAGTTGCCGTATTCGT
hu TMEM63A-578-F	CATCCACAGTCCTTCCTTCCC	hu TMEM63A-722-R	TGTAGCAATAGGAGTCGTTGGG
hu TMEM63B-432-F	GCAGGAGAGGGACCGAGTG	hu TMEM63B-516-R	AGAGGTGAGACGCTCATACCG
hu TRPC1-911-F	GAGGAACTAGCCCGGCAATG	hu TRPC1-1019-R	GAGGCTCGTCACTAGACGTA
hu TRPM7-1580-F	AGTGGCTGGTTGGATCCTTG	hu TRPM7-1706-R	TCCAGTCTCGGAATGGTAAGG
hu TRPV4-652-F	CATCTACGGGGAAGACCTGC	hu TRPV4-768-R	TGAACTCCCTCATGTTGCCG
hu ANXA5-633-F	CCTTCAGGCTAACAGAGACCC	hu ANXA5-728-R	CCCCATTTAAGTTCTCCAGCC
rat Piezo1-710-F	ACGCCTCACAAGGAAAGCC	rat Piezo1-858-R	CCGTGATCCGGAAGCGA
rat Piezo2-426-F	CCTGGCGGTCTTTAGCTCAC	rat Piezo2-500-R	GTGTCTGGGCGGCGTAG
rat Pkd2-137-F	GGGGCCTGGAGATTGAGAT	rat Pkd2-262-R	GGTTGTCGCGGCTCCAT
rat Anxa5-526-F	TCCTCCTTCAGGCCAATAGAG	rat Anxa5-642-R	ACTTTTCTTCATCCGTCCCCC
rat Gapdh-50-F	AGTGCCAGCCTCGTCTCATA	rat Gapdh-180-R	GAAGGGGTCGTTGATGGCAA